Optimizing RGB Lighting for Lettuce Growth in Vertical Farms With Bio-Inspired Optimization Algorithm

Rafael Gomes Alves, Fábio Lima, *Member, IEEE*, Ítalo Moraes Rocha Guedes, and Salvador Pinillos Gimenez, *Senior Member, IEEE*

***Abstract*—Vertical farming offers a controlled environment for food production in regions where land scarcity and environmental stress are prevalent. This study presents a bio-inspired optimization strategy for refining the spectral composition of red, green, and blue (RGB) light from light-emitting diode (LED) to enhance crop performance. A genetic algorithm (GA) was employed to iteratively adjust spectral ratios in 2.5-day intervals over a single 25-day practical growth cycle. The algorithm employed selection, crossover, and mutation operators, targeting a weighted-sum fitness function based on key morphological traits, including fresh weight, height, width, and the number of leaves. An experimental trial was conducted under controlled conditions, with identical light intensity and photoperiod for both RGB treatments and a cold-white LED reference. The primary finding is that the optimization process successfully converged on a stable composition of approximately 67% red, 13% green, and 20% blue, which is consistent with prior studies on photosynthetic efficiency. This convergence validates the GA's ability to autonomously discover a scientifically backed recipe from a neutral baseline. A final statistical analysis of the individual plant traits revealed a complex, multiobjective response, with plant height being the most statistically responsive parameter, while differences in the final biomass and leaf count were not statistically significant under the tested conditions. These findings demonstrate the potential of evolutionary algorithms for solving complex, multiobjective optimization problems in vertical farming, supporting the development of adaptive lighting strategies.**

***Index Terms*—Artificial lighting, controlled environment agriculture (CEA), genetic algorithm (GA), optical composition, optimization algorithm, vertical farm.**

I. Introduction

AGRICULTURE serves as the predominant food source for humans and can potentially mitigate global hunger while promoting economic development in emerging economies [1], [2]. However, the sustainability of current agricultural practices is increasingly scrutinized due to the increasing strain on Earth's resources [1], [2]. Furthermore, it is expected that the global population will reach its peak at about 10.3 billion during the mid-2080s before decreasing to nearly 10.2 billion by 2100, with a strong probability that this peak will occur within this century [3]. Hence, it is crucial to expand agriculture under sustainable conditions to effectively address the challenges of climate change and maintain food security [4], [5].

In response to the increasing global population, urban expansion, decreasing agricultural land, food supply shortages, and the decline in agricultural labor, it is urgently necessary to maximize the use of increasingly limited arable land and to provide food-producing alternatives to sustain the growing population [6]. In this regard, vertical farms, also known as plant factory with artificial lighting (PFAL) or indoor farming [7], [8], offer a promising solution to increase food production in regions with limited land or challenging environmental conditions by enabling food production in urban centers, repurposing underutilized urban infrastructure and addressing problems typical of large metropolises, such as food deserts [9], [10], [11], [12].

However, vertical farming faces significant challenges, especially with regard to high initial investment and operational expenses [13], [14], [15], [16], [17]. The primary expenditures are derived from the consumption of electrical energy for climate control and lighting [13], [15], [18], [19]. The consumption of electric energy in vertical farms is mainly driven by environmental control and the requirement to provide photosynthetically active radiation (PAR) to the plants. Therefore, to achieve more sustainable vertical farming, it is essential to improve light use efficiency (LUE), defined as the mass of commercially available fresh produce per unit of incident light energy ($g \cdot mol^{-1}$) [7], [13].

In this study, we aimed to use a bio-inspired optimization algorithm to dynamically adjust the spectral composition of light from red, green, and blue (RGB) light-emitting diode (LED), focusing on RGB spectra, while maintaining constant light intensity for optimal lettuce growth. This algorithm functions as a decision-making microservice in the Internet of Things (IoT) platform we previously described [20]. To assess its efficacy, we measured crop variables such as plant height, width, fresh weight, and leaf count over time, comparing them

Received 22 August 2025; revised 26 November 2025; accepted 11 December 2025. Date of publication 17 December 2025; date of current version 23 February 2026. This study was financed in part by the Coordenação de Aperfeiçoamento de Pessoal de Nível Superior—Brazil (CAPES) - Finance Code 001. The work of Salvador Pinillos Gimenez was supported in part by the Conselho Nacional de Desenvolvimento Científico e Tecnológico (CNPq) under Grant 304427/2022-5 and in part by the Fundação de Amparo à Pesquisa do Estado de São Paulo (FAPESP) under Grant 2020/09375-0. *(Corresponding author: Rafael Gomes Alves.)*

Rafael Gomes Alves is with the Department of Computer Science, Centro Universitário FEI, São Bernardo do Campo, São Paulo 09850-901, Brazil (e-mail: ralves@fei.edu.br).

Fábio Lima is with the Department of Industrial Engineering, Centro Universitário FEI, São Bernardo do Campo, São Paulo 09850-901, Brazil.

Ítalo Moraes Rocha Guedes is with Embrapa Vegetables, Brasília 70770-901, Brazil.

Salvador Pinillos Gimenez is with the Department of Electrical Engineering, Centro Universitário FEI, São Bernardo do Campo, São Paulo 09850-901, Brazil.

Digital Object Identifier 10.1109/JIOT.2025.3645491

to results from cool white light. This study's primary goal was to identify the ideal spectral composition of RGB LEDs for optimal light conditions for lettuce. This approach aligns with the growing trend of applying artificial intelligence (AI) to IoT systems, digital twin (DT), and machine learning models to create autonomous and optimized controlled environment agriculture (CEA) systems [21], [22], [23].

This study is a direct and necessary scientific validation of the conceptual framework proposed in our prior work [20]. That preliminary study focused on the software architecture and feasibility of an IoT-driven DT, proving that a "physical-in-the-loop" genetic algorithm (GA) could run for 34 days. However, that work had a critical scientific limitation: it optimized raw 0–255 RGB values and did not assess or normalize for the photobiological metric of photosynthetic photon flux density (PPFD) (light intensity), making its results hardware-dependent and not scientifically reproducible.

The novel contributions of this article are, therefore, threefold.

1) *Methodological Rigor:* The entire experiment is built upon a constant, validated 200-μmol/m^2 . s PPFD. This ensures all spectral ratios are scientifically comparable and directly fix the primary flaw of the previous work.
2) *Refined Optimization:* The GA's fitness function is advanced from a simple average to a weighted-sum model, prioritizing commercially valuable traits (e.g., 0.5 for fresh weight).
3) *Full Statistical Validation:* This work provides a complete statistical analysis (Welch's *t*-test) of the biological outcomes (weight, height, width, and leaf count) against a control, a rigorous analysis that was absent in the previous work.

Finally, while we acknowledge the value of benchmarking against other algorithms [e.g., particle swarm optimization (PSO)], this "physical-in-the-loop" system requires a 2.5-day practical growth period for a single fitness evaluation. A fair benchmark would necessitate multiple, separate 25-day growth cycles, a significant long-term experimental project. Therefore, the contribution of this work is the first rigorous scientific validation of this GA-based methodology, which was a necessary prerequisite for future comparative studies.

II. Literature Review

This section outlines the basic concepts employed by this study. Section II-A examines crucial features of vertical farming, including the light energy properties and their impact on plant growth. Section II-B explores key ideas associated with the bio-inspired optimization algorithm of AI.

A. Vertical Farming

According to the published literature, the main purpose of vertical farming is to improve the productivity of food production while minimizing ecological impacts in urban settings [8], [10], [24], [25], [26]. Benke and Tomkins [8] further emphasize that vertical farms offer significant advantages, such as year-round production, increased yield per unit area, and avoidance of environmental stressors such as droughts, floods, and pests, due to their operation in controlled environment conditions. Moreover, Al-Kodmany [27] categorizes vertical farms into three main types: Type I, which involves repurposed high-rise structures with stacked grow beds; Type II, which refers to rooftop farms; and Type III, which includes innovative multilevel designs. It should be noted that several authors, such as Kozai et al. [7] and Shamshiri et al. [28], refer to Types I and III as PFAL.

Fig. 1. Vertical farm as demonstrated in the Aerofarms facility [29].

As described by Kozai et al. [7], a vertical farm system typically includes the following:

1) a thermally insulated space;
2) multitiered cultivation shelves with artificial lighting;
3) a closed-loop water system for nutrient solution management;
4) an integrated ventilation and air-conditioning system;
5) an optional carbon dioxide (CO_2) supply unit;
6) a control unit dedicated to monitoring production parameters to achieve optimal productivity and food quality.

Fig. 1 illustrates a vertical farm example with vertically arranged grow beds within a building under controlled environment conditions.

An essential component of vertical farming involves the use of artificial lighting to provide the energy required for photosynthesis [7], [30]. However, the influence of light on plant growth is varied because each species, and even cultivars within one species, reacts distinctively according to its specific characteristics [30].

Traditionally, the wavelength range spanning from 400 to 700 nm, known as PAR, plays a crucial role in influencing crop growth and development. However, recent studies indicate that other wavelength ranges, such as extended PAR (ePAR) ranging from 400 to 750 nm, and the photobiologically active radiation (PBAR) ranging from 280 to 800 nm, also hold considerable potential for influencing crops [31], [32], [33], [34].

Bantis et al. [30] underscore that a wide array of studies have investigated different combinations of light energy, covering spectra from ultraviolet (UV) (280–400 nm) to far-red (700–800 nm) across various species. Additionally, the authors point out that: 1) ratios of red/blue and red/far-red

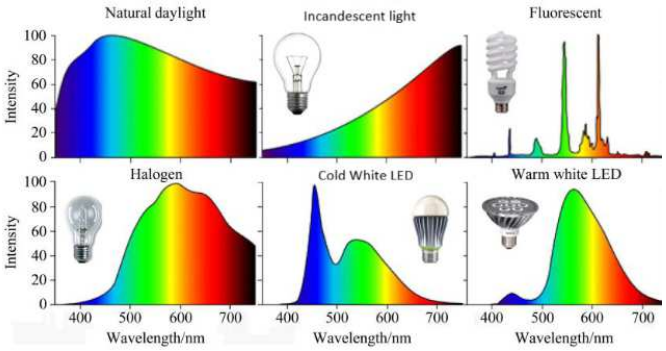

Fig. 2. Intensities of spectral power distribution of natural and different artificial light sources according to [28].

light are crucial in modulating and determining the growth of higher plants; 2) the light energy of the blue spectrum significantly enhances the production and accumulation of phytochemicals such as phenolics, carotenoids, and volatiles, leading to increased plant antioxidant activity; and 3) although UV radiation is not widely applied in horticulture, its influence on plant development and secondary metabolism, particularly UV-A (315–400 nm) at low doses, may be harnessed to produce compact and high-quality plants.

This suggests that no single light spectrum and intensity works best for all cultivars, making it challenging to determine the ideal light characteristics for a specific crop [35], [36], [37]. Multiple studies, for example, analyze the impact of different light compositions, intensities, and strategies on lettuce, highlighting that growth responses vary significantly depending on the cultivar and environmental conditions [35], [38], [39], [40], [41], [42]. These studies often compare combinations of red, blue, and far-red wavelengths, as well as dynamic lighting schedules and supplemental lighting techniques, revealing complex interactions that influence photosynthesis, morphology, and yield.

Published research suggests that the conventional method to define the characteristics of artificial light energy involves specifying PPFD, photoperiod, and daily light integral (DLI) [7]. PPFD refers to the count of photons that impact a surface area of 1 m^2/s, measured in μmol/m^2 . s [7]. The photoperiod refers to the duration of light exposure that a plant receives within a 24-h cycle. Lastly, DLI quantifies the total amount of PAR received over 24 h, and is considered as the total number of photons collected over a day on a surface area of 1 m^2, expressed in mol/m^2day and illustrated in the following equation [7]:

$$\text{DLI} = \frac{\text{PPFD} \cdot \text{photoperiod} \cdot 3600}{1\,000\,000}. \tag{1}$$

Variables such as PPFD and DLI can differ substantially depending on the type of artificial light energy and its proximity to the crop canopy. Consequently, considering these variations is crucial during assessments and optimizations to guarantee that the findings are precise and relevant for each particular lighting source setup. In addition, each artificial light source possesses different characteristics. Fig. 2 depicts the intensities of spectral power distributions of different lighting sources as a function of the wavelength/nm [28].

B. Genetic Algorithms

GA, a subset of evolutionary computing, is a heuristic evolutionary algorithm capable of optimizing complex systems characterized by a multitude of input and output variables, often referred to as specifications. This bio-inspired optimization algorithm is predominantly applied in the search, optimization, and machine learning contexts [43], [44].

GA draws on Darwin's concept of survival of the fittest [45], [46] and uses biologically inspired operators, including inheritance, selection, crossover, and mutation, to conduct heuristic searches and optimization [45], [47], [48]. Various techniques are available to implement each one of these operators in GA, as detailed in [45], [49], and [50]. Fig. 3 shows the commonly used operators, as noted in [51].

A generic GA functions by manipulating a population of candidate solutions created randomly, beginning with the evaluation of an initial set of chromosomes, also called individuals. Each chromosome consists of multiple genes, defined by the input variables, which numerically encode a proposed solution to a particular problem. The fitness of each solution, defined by each chromosome, is determined, and the chromosome with the most elevated performance is selected for reproduction. Mutation and crossover processes introduce genetic variability into the population of the next generation to be evaluated, helping to evolve toward optimal solutions. Adequate design and parameter optimization of the GA can enhance the probability of reaching a global optimum within a feasible number of iterations [51].

GAs have also been applied to the agricultural sector, encompassing areas such as crop management, irrigation systems, and soil analysis [52]. To the authors' knowledge, the use of GA to optimize light spectral composition generated by RGB LEDs in vertical farming crop growth has not been thoroughly investigated and was initially presented in our previous study [20]. In this investigation, binary encoding is employed for each spectral composition produced by the RGB LEDs. Single-point crossover is applied during the reproduction process, and bit-flipping mutation is used in the mutation process. The selection process is designed to favor only the most suitable candidate, as there is only a small number of candidates per population. Comprehensive information on the algorithm and its features is available in Section IV.

C. IoT Platform and GA Integration

Integrating the IoT with AI is crucial for enhancing precision agriculture, facilitating data-driven improvements in crop yield and resource management [22], [23], [53], [54]. This research was performed on an existing IoT-supported vertical farming system. The system employs a multilayer architecture using the FIWARE framework [55] to handle real-time data from various environmental sensors [53], [56]. Data are relayed via message queuing telemetry transport (MQTT) to a central Orion Context Broker (OCB) for context management and processing [57], [58].

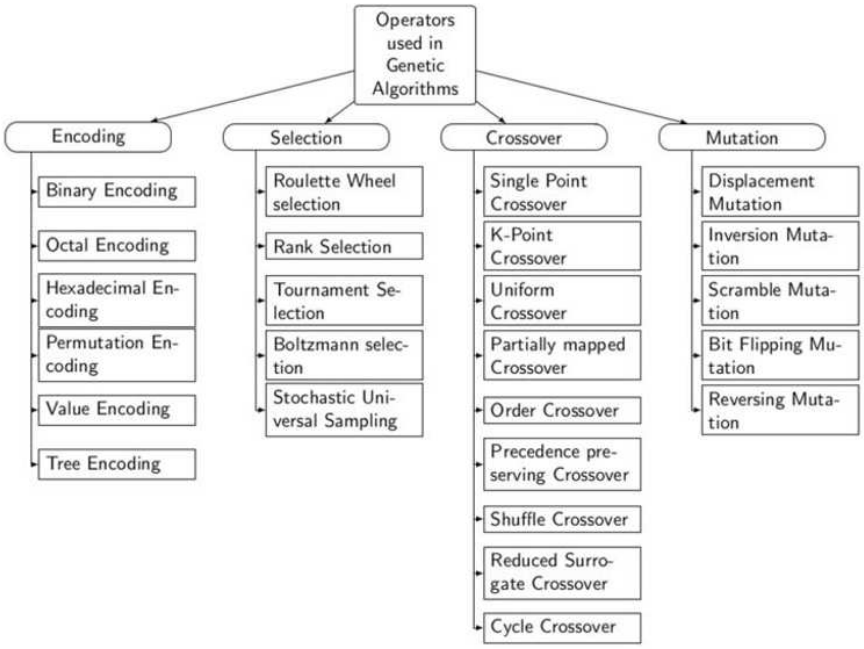

Fig. 3. Operators used in GA according to [51].

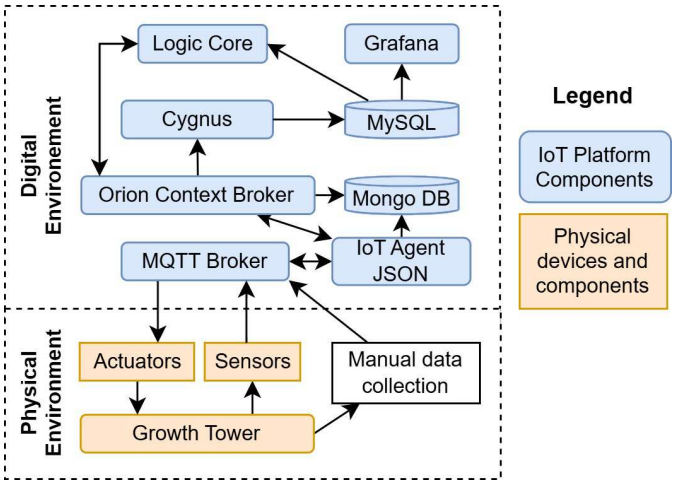

Fig. 4. Simplified IoT architecture from [20], highlighting the data flow between the physical layer, the OCB, and the GA-driven logic core.

Expanding upon this foundation, we present an advanced decision-making component, situating the system within the artificial Intelligence of Things (AIoT) framework [59], [60]. Termed the logic core, this component functions as a microservice that incorporates a GA to autonomously enhance the lighting environment. It systematically processes real-time sensor data from the OCB, historical patterns derived from a MySQL database, and manual crop measurements (e.g., biomass and height) to formulate optimal lighting recipes.

Initially developed as a prototype and thereafter deployed as a scalable application programming interface (API), the logic core functions within a closed-loop system. Upon collection of new manual crop data, it initiates queries to the OCB to access pertinent historical data. Thereafter, it utilizes the GA to derive an optimized light recipe and dispatches updated lighting configurations, new RGB values, as actuation commands to the OCB. These directives are then transmitted via MQTT to dynamically modulate the light fixtures within the growth tower, exemplifying an automated sense-analyze-actuate cycle designed for precision crop management akin to the functionalities in [56] and [61]. An abbreviated diagram of this architecture is illustrated in Fig. 4.

III. Experimental Setup

Fig. 5 illustrates the experimental physical structural setup of the vertical farm prototype evaluated in this study. The growth tower comprises four tiers, of which three tiers are equipped with RGB fixtures containing RGB LEDs (Taiwan Brand Chip Epistar: red 620–625 nm, green 520 nm, and blue 460 nm), while the remaining tier employs exclusively cold-white LEDs (Taiwan Brand Chip Epistar: cold white 10 000 K). This cold white LED was chosen as the reference control for two primary reasons. First, its broad-spectrum output (see Fig. 2) provides photons across the entire PAR range, serving as a robust, nonoptimized baseline that includes all necessary *R*, *G*, and *B* wavelengths. Second, it represents a common, low-cost default lighting solution used in many nonoptimized commercial and hobbyist systems [35]. Therefore, the goal was not to benchmark against a predefined best literature recipe, but rather to use this full-spectrum baseline to test if the GA methodology could autonomously discover an optimized recipe from a neutral starting point.

An opaque divider separates each RGB-lit shelf into two separate lighting zones. Consequently, there are six distinct RGB lighting zones and one control zone illuminated by cold-white light. Each RGB lighting zone can hold up to four plants, while the cold-white lighting zone can hold up to eight plants;

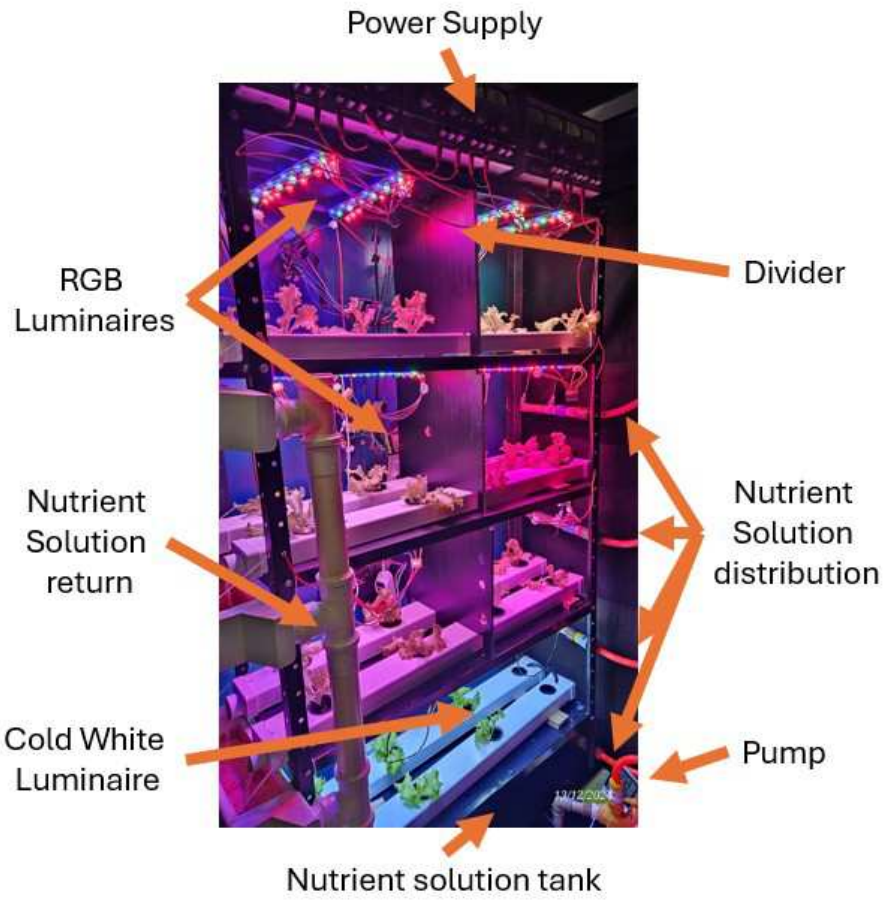

Fig. 5. Experimental physical structural setup of the vertical farm prototype used in this study.

however, only six were used. In addition, an air-conditioning unit was employed inside the growth tower to maintain a constant temperature of approximately 24 °C ± 1° and optimal humidity levels within the growth tower.

The IoT platform's hardware and firmware (first introduced in [20]) were implemented as follows. The primary control and data aggregation for the growth tower were managed by a server running the Ubuntu Server operating system, which hosted the MQTT broker and the IoT platform's services. Each of the six RGB lighting zones and the one cold-white zone was individually actuated by an ESP32 microcontroller using the MicroPython framework. These microcontrollers drove the luminaires via custom-designed LED driver boards using 12-bit pulsewidth modulation (PWM) signals to ensure precise current regulation and spectral mixing.

For sensing, environmental data such as air temperature and humidity were monitored using calibrated DHT22 sensors connected to the local microcontrollers. The nutrient solution's electrical conductivity was manually monitored with a B-MAX TDS/EC meter, and the light intensity (PPFD) for all zones was validated and calibrated using a Goyojo PAR Meter GT121. Regarding communication, all devices reported data via MQTT to the central OCB. In this local network environment, round-trip communication latency was consistently under 500 ms. Given that the GA's actuation intervals were 2.5 days, this level of performance and reliability was more than sufficient for the study's requirements.

Lettuce (*Lactuca sativa var. crispa*) was chosen as the main crop for this study due to its prevalence in vertical farming systems [7]. A hydroponic system was used to supply nutrients to the crops. A 130-L reservoir was used to store and distribute the nutrient solution to all the plants used in this study. The nutrient solution was evenly distributed across the shelves through a water pump, which operated for 15 min every hour, and a four-way water splitter valve. The nutrient solution consisted of a mixture of all the essential macro and micronutrients (flex blue and flex red mineral nutrients from PlantPar), prepared according to the manufacturer's guidelines, with the aim of reaching an electrical conductivity, measured by a digital TDS/EC meter (*B*-MAX), of approximately 1.5mS/cm, which is suitable for lettuce cultivation. The nutrient solution was prepared using tap water, with the pH value of 6.18 determined via a calibrated hydroponic pH meter (Ruolan).

To establish the reference light energy intensity, the PPFD in the reference zone was measured using a quantum sensor (Goyojo PAR Meter GT121), yielding an approximate value of 200 μmol/m^{-2} . s^{-1}. This value was used as a reference to validate the RGB lighting zones with the same sensor during the experiment, as described in Section IV. All plants in the proposed methodology were subjected to a 16-h photoperiod.

Before starting the experiment, ten-day-old lettuce seedlings, acquired from a horticultural supplier in a 100-cell tray, were transplanted to the growth tower. Seedlings with similar initial morphologic characteristics were randomly selected from this tray for transplantation, after which they underwent a five-day acclimation period under cold-white light energy. Data on fresh biomass, height, width, and the number of leaves were collected approximately every 2.5 days for use in the proposed methodology (Section IV). The experiment lasted 25 days, including the acclimation phase. As the experiment began with ten-day-old seedlings, followed by a five-day acclimation period, this 25-day experimental period resulted in a total seed-to-harvest growth cycle of 40 days, which is a standard, commercially relevant duration for hydroponic lettuce. This duration was chosen because, at this point, the crops reached their maximal size that could fit within the growth tower without shoot overlap. This 25-day duration constituted one complete, practical growth cycle. This single cycle was divided into 2.5-day evaluation periods. Each period represented a single "generation" of the GA, where practical trait data were collected to inform the next iteration of the algorithm, as detailed in Section IV.

The fresh biomass of the plants, including the substrate and net pot weight, was determined with a digital balance (MH-500). To standardize water content for crop weight assessment, the entire crop substrate was immersed in the nutrient solution until saturation, followed by a standard drainage period of 10 s prior to measurement to remove excess gravitational water. The height was measured from the surface of the substrate (stem base) to the top of the tallest leaf using a digital caliper (Bomder). The width was measured from the center of the substrate/crop to the tip of the furthest leaf using the same digital caliper. The number of leaves was counted by visual inspection. These indicators were used to calculate the fitness metric for varying RGB spectral composition within each of the defined RGB lighting zones, as detailed in Section IV-A.

IV. Proposed Methodology

The GA presented in this investigation is depicted in Fig. 6. This algorithm seeks to optimize the spectral composition of the light energy generated by RGB LEDs aiming to enhance the crop performance metrics such as height, width, fresh biomass, and the number of leaves. Grounded in Darwin's survival of the fittest principle [45], it evaluates each spectral composition of the RGB LEDs in relation to the cold-white light spectrum. This methodology exhibits minor variations from that described in [20]. Within the context of this article and experimental setup, the proposed GA consists of ten distinct stages, outlined as follows.

1) *Initialize Population Randomly:* A preliminary population of random individuals, referred to as the first generation, is generated. Each individual consists of a chromosome that is defined by three genes, in which each gene represents a percentage (ranging from 0% to 100%) of the reference PPFD value. In this study, the reference PPFD corresponds to the light intensity over the area that is illuminated with cold-white light energy, which was previously measured as 200 μmol/m^{2}s. To ensure that the maximum PPFD for each specific lighting zone aligns closely with the reference value, these percentages must be normalized, so the sum adds up to 100. The population size is determined by the number of RGB light energy zones, which, in this experiment, is set to six.
   It is important to note that this initial population was generated completely at random and was not seeded with predefined optimal recipes from the existing literature. This was a deliberate methodological choice. The primary objective of this study was not merely to find an optimal recipe, but to validate the GA's ability to autonomously discover an optimal solution from a neutral, unbiased starting point. Seeding the initial population with known high-performance (e.g., high-red) recipes would have introduced human bias and prevented a true test of the algorithm's exploratory and convergence capabilities. A random start ensures the entire search space is available for exploration from the beginning.
2) *Actuation:* Every member of the population is allocated to one of the six distinct RGB light energy areas, labeled as 1 Left, 1 Right, 2 Left, 2 Right, 3 Left, or 3 Right. The intensity of each RGB spectral composition is constrained by the corresponding gene in the individual's chromosome. A quantum sensor measures the PPFD for each RGB spectral composition, as well as for the entire lighting area, to verify that the intensity matches the reference PPFD value within a specified tolerance of 5%. Additionally, environmental variables such as temperature, humidity, and nutrient solution electrical conductivity are kept stable across all lighting zones during the experiment through the use of an air conditioner and the same nutrient solution for all lighting zones.
3) *Fitness Evaluation:* Every 2.5 days, on average, measurements of the crop's fresh biomass, height, width, and the number of leaves are recorded. After collecting these data, the performance of each lighting zone is assessed through a fitness evaluation, as detailed in Section IV-A. This process helps identify the best individual for a given generation.
4) *Generate a New Population:* After evaluating the first generation a new population, called the "second generation," is generated. This population consists of individuals with combined genes from random individuals and the best individual from the first generation. The selection, crossover, and mutation operators of traditional GA are used in this stage. Finally, a validation step is then conducted to ensure compliance with constraints. A detailed process to create this new population is indicated in the next items.

   a) *Selection of the Best Individual:* The individual with the top fitness score, indicating optimal performance according to the problem's objective function, is ensured to transmit its genes to the subsequent generation, thus preserving the best

solution identified thus far. The fitness score function is described further in Section IV-A.

b) *Generate New Random Individuals:* To maintain genetic diversity and explore the sample space of potential solutions (other individuals), a new random population is generated. At this stage, there is no requirement for the number of individuals to match the number of zones illuminated by the RGB LEDs in the experimental setup.

c) *Crossover:* The genetic material of the top-performing individual, identified through the analysis of the prior population (previous generation), is combined with newly generated random individuals. This integration seeks to produce offspring with novel gene combinations representing new RGB spectral composition, which may improve the cultivar's features in the next evaluation. This study uses one-point crossover as described in Section IV-B1.

d) *Mutation:* To further explore the diversity enhancement, minor random modifications in each gene of each individual are applied. This study uses bitwise mutation, with a comprehensive procedure outlined in Section IV-B2.

e) *New Population:* Finally, a new population of individuals is created after the selection, crossover, and mutation process. The number of individuals in this new population is the same as in 4b), and is not restricted to the number of lighting zones available in the experimental setup.

f) *Validation:* In contrast to standard GA, every individual in the emerging population is subject to a validation process to verify compliance with necessary constraints. Specifically, the sum of genes for each individual is required to be 100, necessitating a normalization procedure for each individual. Additionally, this stage allows for integrating expert knowledge in the validation procedure, allowing for small changes to be made in each individual if needed. Notably, this study did not employ expert knowledge for validation.

5) *Final New Population:* The final new population size is modified based on the six lighting zones available in the experimental setup. The best individual from the previous population remains in its respective zone, while additional candidates are randomly chosen to fill all potential lighting zones. This approach guarantees a representative and efficient group of candidates for each generation. These selected candidates are used to adjust the spectral composition generated by the RGB LEDs of each lighting zone within the growth tower, restarting the process at stage 2.

Detailed explanations of the fitness evaluation, crossover, mutation, and validation procedures used in the proposed GA are presented in Sections IV-A and IV-B. A complete summary of all quantitative parameters used for the GA, such as population size, mutation rates, and fitness weights, is provided in Table I for reproducibility.

TABLE I
SUMMARY OF GA CHARACTERISTICS

Parameter	Value / Description
Population Size	6 individuals
Initial Population Strategy	Random Initialization
Intermediate Population Size	5 times the number os lighting zones
Selection Method	Elitist Selection (the best individual is retained)
Encoding	8-bit binary (for crossover & mutation steps)
Crossover Type	One-point crossover
Mutation Type	Bitwise mutation (bit-flipping)
Mutation Rate	5%
Normalization	Gene sum for each individual is normalized to 100, representing 100% of a $200 \mu mol/m^2 s$ PPFD
Fitness Function	Weighted sum of 4 traits: 0.5 to Fresh Weight, 0.1 to Height, 0.1 to Width and 0.3 to Number of Leaves
Stopping Criterion	Fixed 10 generations (intervals) over a 25-day practical growth cycle

To clarify the experimental procedure, it is essential to distinguish between the practical growth cycle and the algorithmic generations. The methodology was executed over a single, continuous 25-day practical lettuce growth cycle. The experiment was not simulated, nor did it involve multiple, separate 25-day growth cycles.

The generations of the GA, as described in this section, correspond to the 2.5-day measurement intervals within this single experiment. At the end of each 2.5-day interval, practical measurements (fresh weight, height, etc.) were collected from the real plants. This real-world data were then used as the input for the GA's fitness evaluation (Step 3) to "evolve" and determine the new, optimized RGB lighting configurations for the next 2.5-day physical growth interval (Steps 4 and 5).

A. Fitness Evaluation Procedure

A pseudocode representation of the process to assess the fitness of each individual in a given generation is described in Algorithm 1. Initially, this involves recording the specifications (fresh biomass, height, width, and the number of leaves) of crops across all lighting zones, with measurements spaced 2.5 days apart, on average. Subsequently, the change between these two measurements is computed using (2), where C denotes the variation in a crop characteristic for a specific crop, n indicates the crop number, V represents each characteristic, and t corresponds to the measurement at a particular time point.

$$C_n = V_t - V_{t-1}. \tag{2}$$

Subsequently, (3) is used to define the average change value for each crop feature in each lighting zone. In this equation, A represents the average value for a given light zone and crop characteristic, n denotes the number of crops in the given light zone, and C_n signifies the variation in a specific crop characteristic observed between two consecutive measurements. In this article, n is four for each lighting zone

Algorithm 1 Pseudocode to Calculate the Fitness Value for Each Generation

```
BEGIN
for Each light treatment do
  for Each crop characteristic do
    for Each crop do
      Get value before
      Measure current value
      Calculate the difference between current
      and past values
    end for
    Calculate average value for the differences
  end for
end for
for Each RGB treatment do
  for Each crop characteristic do
    Calculate the difference to the cold white treatment
    Calculate the score considering (max = 100, min = 0)
  end for
  Calculate weighted fitness value based on the scores
end for
END
```

defined by the RGB LEDs and six for the cold-white lighting zone

$$A = \frac{\sum_1^n C_n}{n}. \tag{3}$$

In the subsequent step, for each crop specification, the difference between each lighting zone defined by the RGB LEDs and the reference cold-white lighting zone is taken using (4). Here, D signifies the difference between the average values of a given crop specification, and A represents the average value of a crop specification considering a given RGB lighting zone and the cold-white lighting zone

$$D = A_{\text{RGB}} - A_{\text{Cold White}}. \tag{4}$$

Subsequently, the score for each crop specification is determined using (5), where S denotes the score for a specific crop specification and D signifies the difference between the average values obtained by a particular lighting zone defined by the RGB LEDs and the reference cold-white lighting zone. If the maximum and minimum values of these differences for a given crop specification are equal, the score is assigned a value of 100

$$S = \frac{D - \min(D)}{\max(D) - \min(D)} \times 100. \tag{5}$$

Ultimately, the final fitness value was determined using (6), where F is the final fitness value for a given composition of the light energy intensity of the RGB LEDs, w_v denotes the weight assigned to each specification, and S signifies the score corresponding to that specification. In this study, we assign the normalized weights w_1–w_4 of 0.5, 0.1, 0.1, and 0.3, corresponding to the fresh weight, height, width, and the number of leaves specifications, respectively. These weights were determined based on results from an initial experiment described in [20] and further refined through consultations with vertical farm producers (experts)

$$F = \sum_1^v w_v S. \tag{6}$$

Algorithm 2 Pseudocode for Generating a New Population Using the Previous One and Corresponding Fitness Values

```
Input: population, fitness values
Select the best individual.
Generate new intermediate random population.
Apply crossover between the best individual and the each
individual in the random population.
Apply mutation in the crossover population.
Select, at random, the new candidates based on the number
of available lighting zones.
Ensure that each candidate has genes that sum up to 100.
Place the best individual from the past generation into the
new generation for the same lighting zone.
return New population.
```

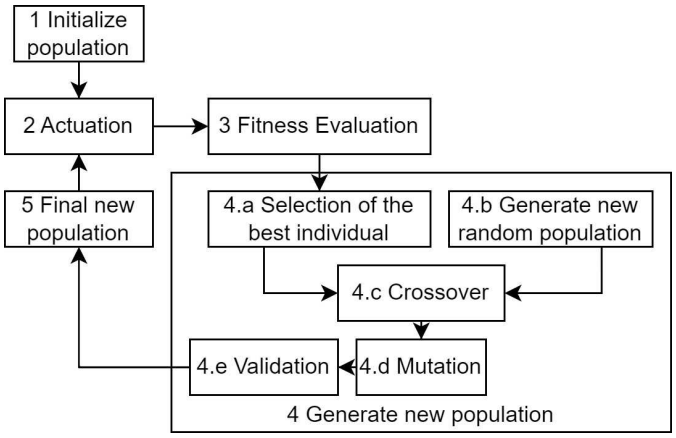

Fig. 6. Proposed GA.

B. Procedure to Generate a New Population

Algorithm 2 generates a new population using evaluated individuals and their fitness scores. The top-performing individual is retained to preserve the best solution from the previous generation. To maintain diversity and prevent early convergence, a randomly generated intermediate population, potentially larger than the number of lighting zones, is introduced. The best individual undergoes a one-point crossover with each member of this population, facilitating genetic exchange. The resulting offspring is subjected to mutation with a specified probability of 5% to avoid local optima. A subset of these mutated individuals is then randomly selected to match the number of available lighting zones. Finally, a validation step ensures that each individual's gene sum equals 100, enforcing existing constraints. The final population consists of the retained best individual and newly generated individuals after selection, crossover, and mutation.

1) Crossover Procedure: In a one-point crossover, the chromosomes of the parent individuals are represented as binary

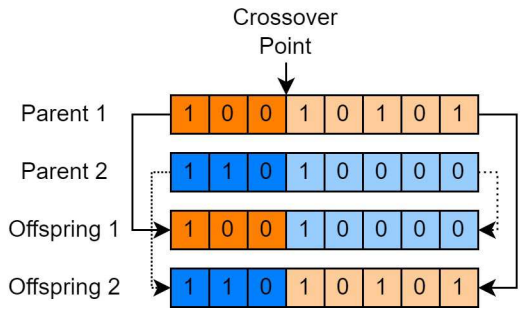

Fig. 7. One-point crossover.

Algorithm 3 Pseudocode to Perform One-Point Crossover

Input: best candidate, random population
Encode the best candidate as binary.
Encode each candidate in the random population as binary.
Initialize an empty crossover population.
for each individual in the random population **do**
Initialize an empty crossover individual.
for each gene in the best candidate and individual **do**
Select a random point for crossover.
Apply crossover getting part of the gene from the best candidate and part from the individual.
Append the crossover gene to crossover individual
end for
Append the crossover individual to crossover population
end for
for each individual in the crossover population **do**
Decode the individual to decimal format.
end for
return crossover population

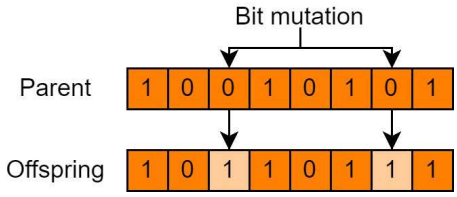

Fig. 8. Bitwise mutation process.

strings consisting of 0 and 1 s. This process employs an 8-bit binary encoding at the outset. Afterward, a random crossover point is selected along these strings. The offspring is generated by combining segments from each parent chromosome, one portion preceding the crossover point and the other succeeding it. This technique produces novel individuals with genetic material inherited from both parents, as illustrated in Fig. 7 [45] and Algorithm 3.

2) Mutation Procedure: Bitwise mutation involves altering random bits within the binary representation of a solution by switching 0–1 and 1–0 s. To allow for this procedure, an 8-bit binary encoding is applied at the outset. This mutation takes place with a specific probability that determines the chance of altering each bit. Fig. 8 shows the bitwise mutation process as described in [45], while Algorithm 4 outlines the method to implement this mutation process.

Algorithm 4 Pseudocode for the Mutation Process

Input: population, mutation rate
Encode each individual in the population to binary format.
Initialize an empty mutated population.
for each individual in population **do**
Initialize an empty mutated individual.
for each gene in individual **do**
Each bit is flipped with a probability equal to the mutation rate.
Append the mutated gene to the mutated individual.
end for
Append the mutated individual to the mutated population
end for
Decode each gene in each individual in the mutated population.
return mutated population

V. Results

This section presents the outcomes of the proposed method and the results for every variable across each RGB LED lighting zone in the experiment (Fig. 5).

A. Results for the Fitness Values for All Generations

Table II illustrates the allocated percentages of light energy spectral composition to the RGB LEDs, together with the fitness scores (Fit) of each lighting zone across various generations. Within each generation, optimal fitness values are marked in blue, while individuals retained from previous generations are denoted in bold black. The light energy spectral composition of the RGB LEDs is expressed as ratios relative to the predetermined PPFD value of 200 μmol/m^2 . s, assuring that the sum for each individual is equal to 100%. The initial generation consists of candidates generated at random, as elucidated in Section IV. It is important to reiterate that this was one continuous practical experiment. Each generation (random, first, second ,. . ., final) listed in Table I represents one 2.5-day interval of real-world growth, not a separate or virtual growth cycle. These sequential intervals sum up to the total 25-day harvesting period for the lettuce crop.

It should be noted that the initial random population (random in Table II) exhibited a well-balanced mixture of individuals, with some displaying a predominance of red, others green, and others blue. From the third generation onward, the red component gained significance and maintained its prominence throughout the process. In particular, in the fourth generation, the optimal individual possessed only red and blue components. However, from the fifth generation onward, the findings suggested that an equilibrium of approximately 65%–70% red, 10%–15% green, and 15%–20% blue yielded optimal results. Ultimately, the results of the proposed methodology indicate that the ideal composition for maximizing performance comprises 67% red, 13% green, and 20% blue.

TABLE II
ALLOCATED PERCENTAGES OF SPECTRAL COMPOSITION OF THE RGB LEDS AND THE FITNESS METRICS RECORDED IN EACH GENERATION

	Random				First				Second				Third				Fourth			
Lighting Zone	**R**	**G**	**B**	**Fit**	**R**	**G**	**B**	**Fit**	**R**	**G**	**B**	**Fit**	**R**	**G**	**B**	**Fit**	**R**	**G**	**B**	**Fit**
1 Left	47	32	21	**66.8**	**47**	**32**	**21**	**85.6**	**47**	**32**	**21**	77.9	2	63	35	54.5	67	4	29	45.0
1 Right	36	31	33	25.7	36	18	46	29.5	28	67	5	63.4	38	46	16	5.6	57	27	16	70.4
2 Left	32	17	51	60.8	36	19	45	65.0	51	32	17	**80.4**	**51**	**32**	**17**	42.2	58	12	30	67.7
2 Right	35	44	21	36.1	79	2	19	52.5	35	33	32	16.0	64	2	34	62.6	80	0	20	**92.9**
3 Left	60	24	16	56.3	47	1	52	21.7	63	2	35	79.3	62	31	7	74.6	54	11	35	67.2
3 Right	48	7	45	30.0	50	39	11	18.7	33	66	1	37.1	60	9	31	**74.9**	**60**	**9**	**31**	0.0
	Fifth				**Sixth**				**Seventh**				**Eight**				**Final**			
Lighting Zone	**R**	**G**	**B**	**F**	**R**	**G**	**B**	**F**	**R**	**G**	**B**	**F**	**R**	**G**	**B**	**F**	**R**	**G**	**B**	**F**
1 Left	81	0	19	57.8	72	13	15	60.0	64	22	14	86.1	53	12	35	60.4	39	8	53	62.9
1 Right	77	10	13	46.1	64	32	4	36.0	54	40	6	40.2	67	15	18	29.9	70	12	18	8.1
2 Left	75	5	20	61.1	62	23	15	55.3	27	30	43	70.4	47	41	12	56.3	30	15	55	57.1
2 Right	**80**	**0**	**20**	59.5	6	47	47	7.2	54	22	24	85.9	60	22	18	59.7	57	27	16	82.7
3 Left	66	17	17	**62.9**	**66**	**17**	**17**	59.0	76	7	17	63.4	67	13	20	**61.4**	**67**	**13**	**20**	**87.7**
3 Right	55	16	29	45.8	69	13	18	**64.4**	**69**	**13**	**18**	**89.2**	**69**	**13**	**18**	5.1	83	12	5	85.9

Analyzing specific generations, the fourth generation strongly preferred red, followed by blue and green. Notably, the final individual in this generation (60:9:31) had a fitness value of zero, indicating the lowest performance across all evaluated variables. This outcome is plausible because fitness values are assessed within each generation rather than across generations. Additionally, since the light composition of each lighting zone was adjusted in every generation, except for the best performer, crops within a given generation may have been at slightly different developmental stages.

An interesting observation arises in the sixth generation, when plants in all lighting zones demonstrated good fitness values except for the "2 Right" lighting zone, which performed the worst. This result is likely due to an insufficient proportion of red light in their spectrum (6:47:47), with a predominance of green and blue. In the eighth generation, the expected least performing crop was "2 Left", given its relatively high proportion of green light at the expense of red. However, contrary to expectations, "3 Right" was the least successful, with RGB proportions of 69:13:18. Since this is the second occurrence of poor performance in this lighting zone, it suggests that other localized environmental variables, such as temperature, humidity, and ventilation, may have influenced the results. Although air-conditioning in the growth chamber stabilizes the overall climate, it can still cause slight variations in each lighting zone's microclimate due to ventilation differences.

These findings do not indicate a continuous increase in fitness between generations, as fitness values are only comparable within the same generation. Instead, they suggest that the evolutionary process progressively favored specific RGB proportions or the development phase of plants.

B. Results for the Biomass Variable

To evaluate the influence of different light energy spectral compositions on plant biomass over time, a comparative time-series analysis was conducted, as presented in Fig. 9. For each lighting condition, the average biomass of plants was calculated at multiple time points and plotted alongside the control group (cold-white LEDs). The treatment and control groups' values are accompanied by error bars representing the 95% confidence interval of the mean. A two-sample *t*-test (Welch's *t*-test [62]) was performed at each time point to statistically assess whether the differences in average biomass between the treatment and control groups were significant. The resulting *t*-statistic and *p*-value are annotated directly on each subplot. Table III presents the final average height for each RGB lighting zone and the reference lighting zone with the difference between them.

TABLE III
FINAL AVERAGE WEIGHTS FOR RGB AND REFERENCE LIGHTING ZONES

Lighting Zone	RGB (g)	Reference (g)	Difference (%)
1 Left	24.9	22.9	8.7
1 Right	21.5	22.9	-1.4
2 Left	24.9	22.9	8.7
2 Right	25.3	22.9	10.5
3 Left	27.2	22.9	18.8
3 Right	21.8	22.9	-4.8
Averages	**24.27**	**22.9**	**6.0**

Based on these results, it is noticeable that crops exposed to an artificial light energy environment provided by RGB LEDs generally outperformed those under cold-white light in terms of average biomass in most lighting zones. In addition, it is noticeable that the treatment "3 Left" had an increase of 18.8%. However, the comparative time-series analysis of crop weight revealed no statistically significant differences between any of the treatment groups and the control group exposed to cold-white LEDs. The Welch's *t*-tests [62] conducted at the final time point for each treatment group resulted in *p*-values well above the conventional threshold of 0.05, indicating that the null hypothesis of equal means cannot be rejected in any case.

These results suggest that none of the alternative lighting treatments produced a significant enhancement or suppression of biomass accumulation in comparison to the control condition. This is further supported by the visual overlap of confidence intervals and the relatively small effect sizes indicated by the *t*-statistics.

From a physiological standpoint, this may indicate that biomass production is either not sensitive to the spectral differences tested or that the duration or intensity of exposure was insufficient to induce measurable differences.

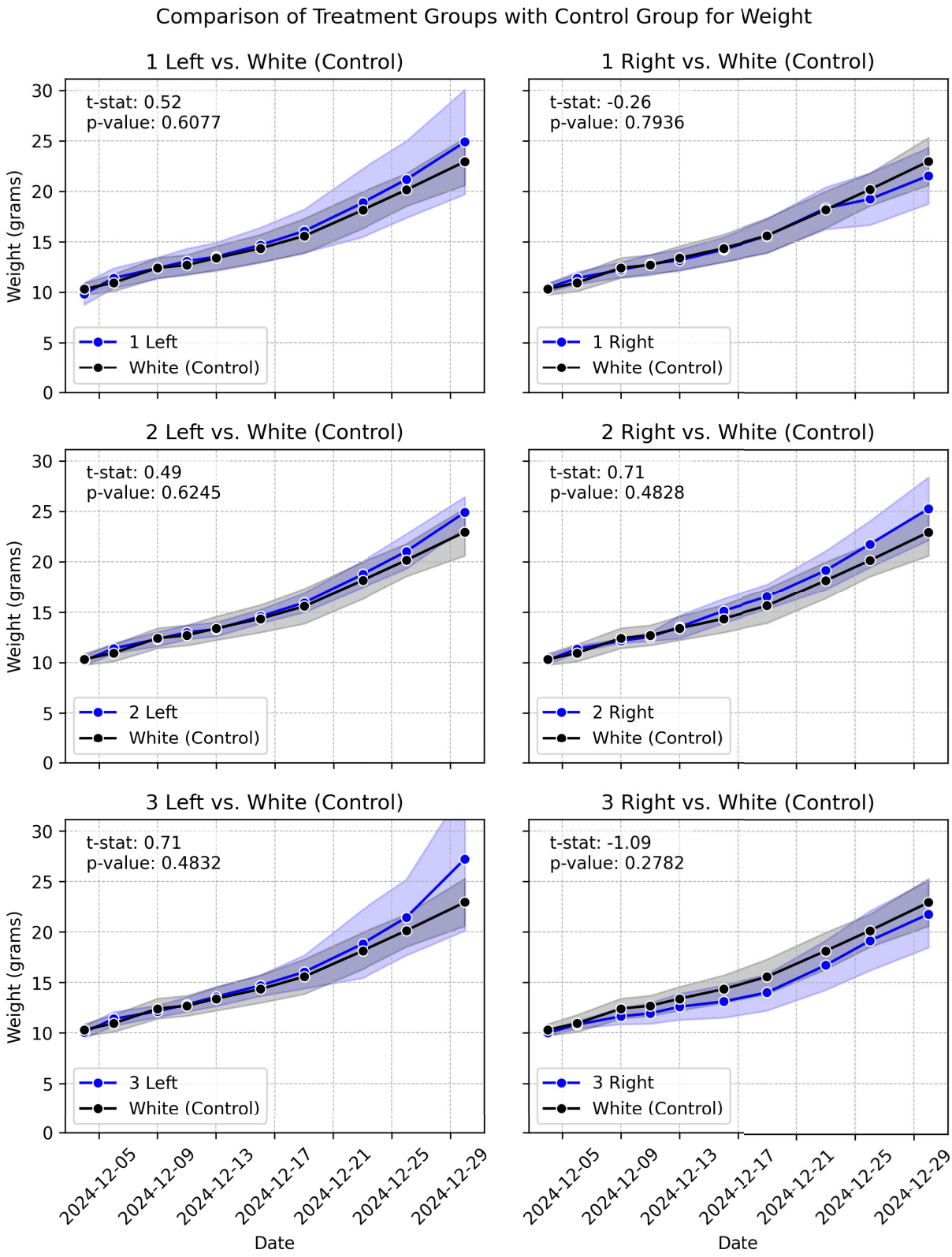

Fig. 9. Average weights over time for each zone illuminated with RGB and cold-white LEDs in the experimental setup.

Another consideration is the high within-group variability, as suggested by the use of standard deviation and confidence intervals. This biological variability may mask subtle treatment effects, particularly if considering the small sample size used in this particular experiment or external conditions that were not controlled in this experiment.

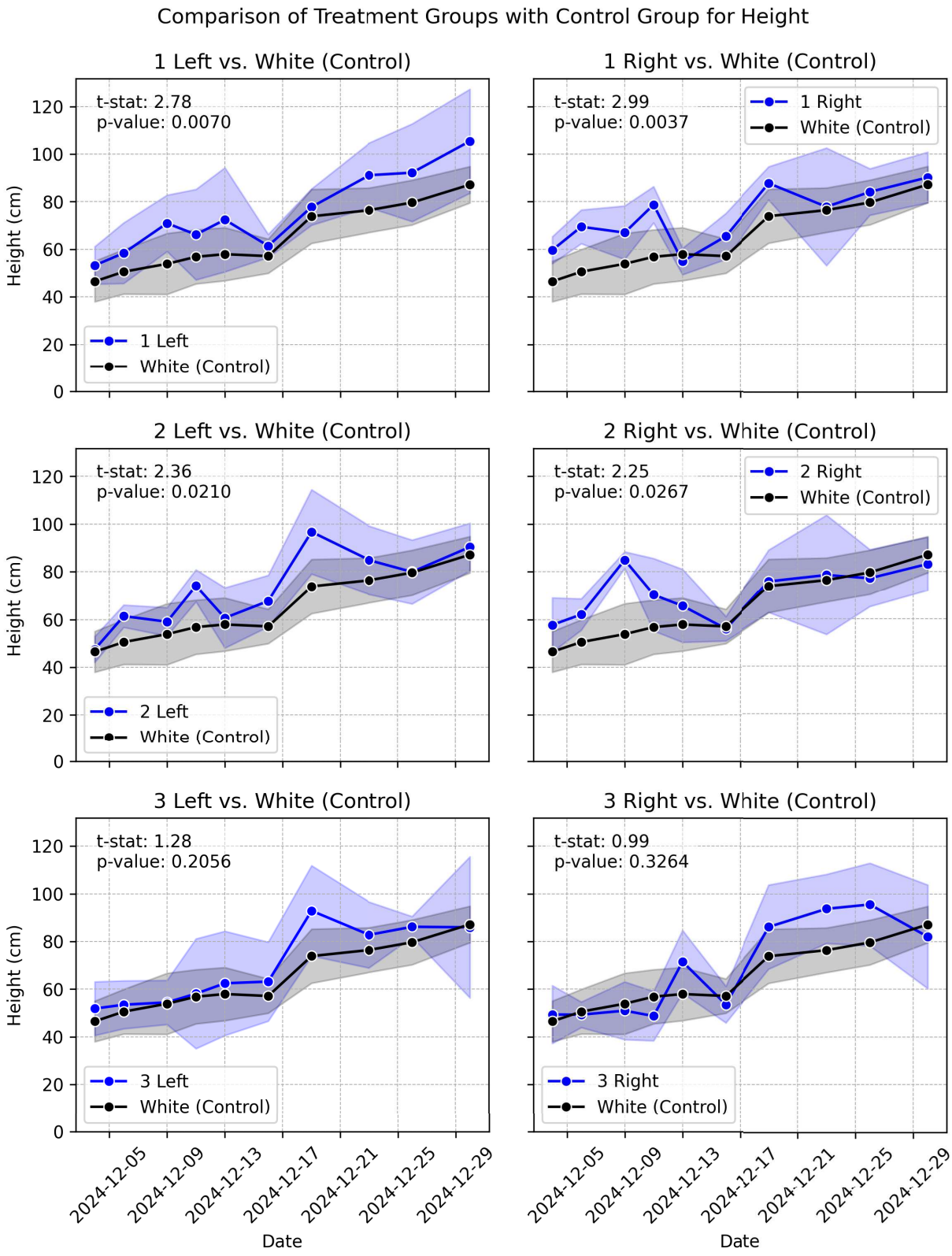

Fig. 10. Average height over time for each group in the experimental setup.

C. Results for the Height Variable

The temporal evolution of plant height under various lighting treatments was similarly analyzed to determine the impact of light spectrum on vertical growth as indicated in Fig. 10. Each subplot compares one treatment group to the control, showing the mean height values at different time points. As in the biomass analysis, error bars indicate the 95% confidence interval for treatment groups and control groups that are presented. Welch's *t*-tests [62] were used to statistically compare

TABLE IV
FINAL AVERAGE HEIGHT FOR RGB AND REFERENCE LIGHTING ZONES

Lighting Zone	RGB (mm)	Reference (mm)	Difference (%)
1 Left	105.5	87.2	21.0
1 Right	90.2	87.2	3.4
2 Left	90.4	87.2	3.7
2 Right	83.2	87.2	-4.6
3 Left	86	87.2	-1.4
3 Right	82	87.2	-6.0
Average	**89.55**	**87.20**	**2.7%**

TABLE V
FINAL AVERAGE WIDTH FOR RGB AND REFERENCE LIGHTING ZONES

Lighting Zone	RGB (mm)	Cold White (mm)	Difference (%)
1 Left	123.3	131.7	-6.4
1 Right	131.6	131.7	-0.1
2 Left	148.6	131.7	12.8
2 Right	138.8	131.7	5.4
3 Left	143.9	131.7	9.3
3 Right	129.2	131.7	-1.9
Average	**135.90**	**131.70**	**3.2%**

the distributions of height values between each treatment and the control. This approach allowed for visual and statistical examination of treatment effects on plant elongation. Table IV presents the final average height for each RGB lighting zone and the reference lighting zone with the difference between them.

This plant feature exhibits significant volatility, as evidenced by the fluctuating data for each crop treatment, primarily due to movement during its measurement. It is evident from Fig. 10 that plants exposed to light energy provided by RGB LEDs generally had a higher average height value than those exposed to the lighting zone with the cold-white color. The comparative analysis of plant height across different lighting conditions revealed statistically significant effects for several treatment groups when compared to the control (cold-white LEDs). Welch's *t*-tests [62] performed at the final measurement point showed that four out of six treatments led to significantly taller plants ($p < 0.05$), suggesting a consistent trend toward increased elongation under specific light spectra.

These results indicate that the light recipes tested in Groups 1 and 2 (both left and right zones) had a significant positive effect on plant height, while Group 3 treatments did not differ significantly from the control.

From a biological standpoint, the observed increase in plant height under certain light treatments may reflect shade-avoidance responses or photomorphogenic effects triggered by the usage of increased red content in the light recipes in these groups.

D. Results for the Width Variable

To assess lateral growth, the width of plants in each lighting zone was monitored and analyzed over time, as presented in Fig. 11. The average width per time point was calculated and visualized for each treatment in comparison to the control group. Error bars denote the variability and reliability of the measurements using confidence intervals (treatment) and standard deviations (control). Statistical significance was tested using Welch's *t*-test [62], and each subplot includes the test statistic and *p*-value to support the interpretation of any observed differences in width between treatment and control groups. Table V presents the final average width for each RGB lighting zone and the reference lighting zone with the difference between them.

The comparative assessment of plant width across different lighting treatments showed limited but potentially meaningful variation in lateral plant development. Among the six treatment groups, only Group 2 Left exhibited a statistically significant difference in width compared to the control group ($p = 0.0444$), as determined by Welch's *t*-test [62]. All other comparisons yielded *p*-values above the 0.05 threshold, indicating no strong evidence of treatment effects in those cases.

Although only one group reached statistical significance, several others (e.g., 2 Right and 3 Left) exhibited marginal *p*-values (<0.1), suggesting a trend toward increased plant width that may become more evident with a larger sample size or reduced variability.

From a biological perspective, increases in plant width may reflect enhanced lateral expansion of leaves or stems, potentially linked to light quality related to blue wavelength. The significant response in Group 2 Left suggests that the spectral composition used across this treatment may have influenced horizontal growth, which could be advantageous for crops where leaf area or canopy coverage is desired.

TABLE VI
FINAL AVERAGE NUMBER OF LEAVES FOR RGB AND REFERENCE LIGHTING ZONES

Lighting Zone	RGB	Cold White	Difference (%)
1 Left	10.8	10	8.0
1 Right	9.58	10	-4.2
2 Left	11	10	10.0
2 Right	10.2	10	2.0
3 Left	10	10	0.0
3 Right	9.8	10	-2.0
Average	**10.23**	**10.00**	**2.3%**

E. Results for the Number of Leaves Variable

The number of leaves per plant was used as a proxy for vegetative development and vigor. This variable was analyzed across the experimental timeline by comparing mean leaf counts between each lighting treatment and the control group, as presented in Fig. 12. Confidence intervals for the treatment groups and standard deviations for the control were included as error bars to illustrate the variation and uncertainty in the measurements. Welch's *t*-test [62] was employed to evaluate statistical differences, and the resulting metrics were annotated within each subplot to guide the interpretation of treatment effects on leaf production. Table VI presents the final average number of leaves for each RGB lighting zone and reference lighting zone with the difference between them.

The comparison of leaf count between different lighting treatments and the control group revealed no statistically significant differences in the number of leaves per plant at the

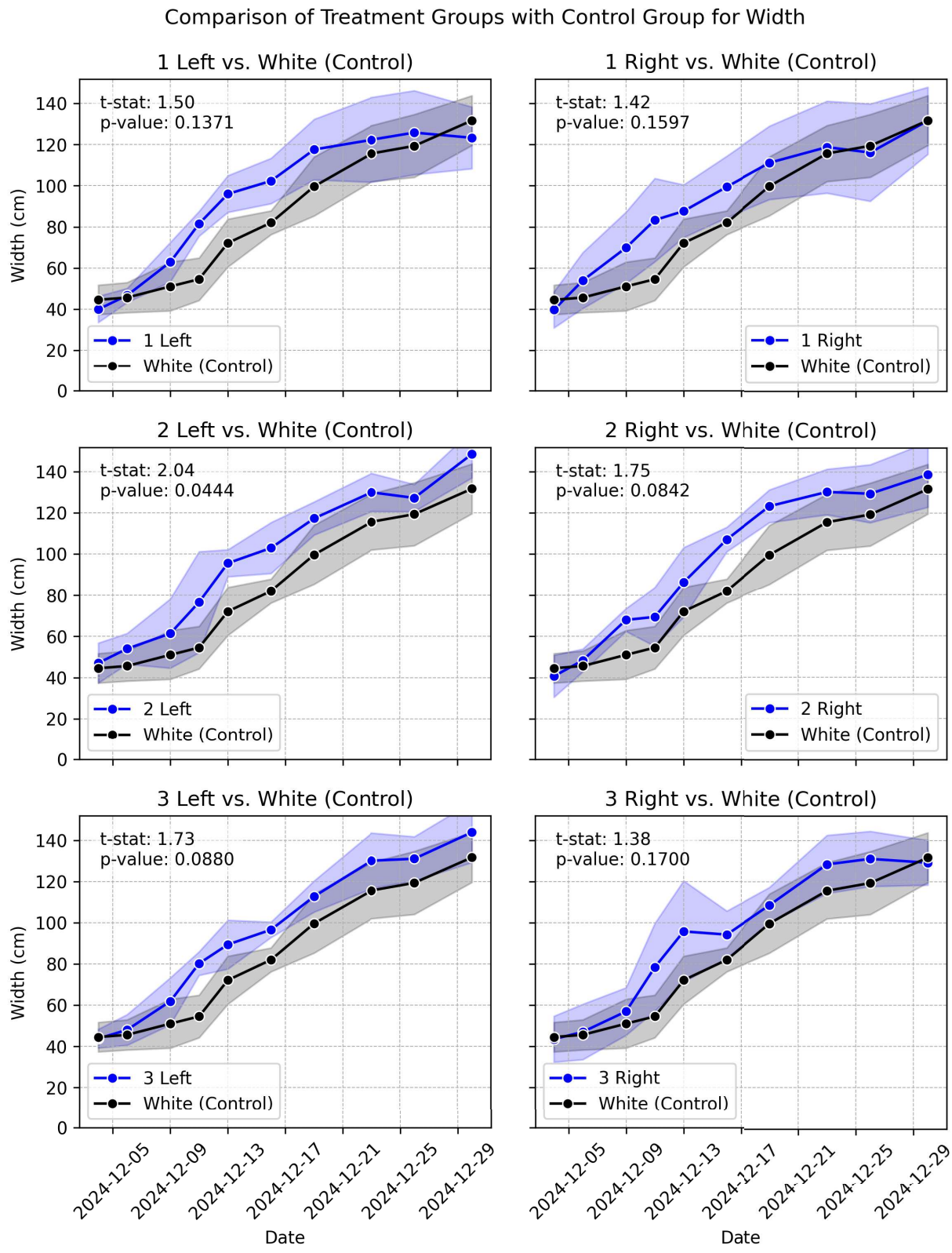

Fig. 11. Average width over time for each group in the experimental setup.

final measurement point. Welch's t-tests [62] for all treatment groups resulted in p-values well above the 0.05 significance level, indicating that the null hypothesis of equal means could not be rejected.

While Group "2 Left" shows a trend toward increased leaf number ($p = 0.0918$), it does not reach statistical significance. The majority of groups display highly similar leaf counts to the control, with values clustered around four leaves per plant.

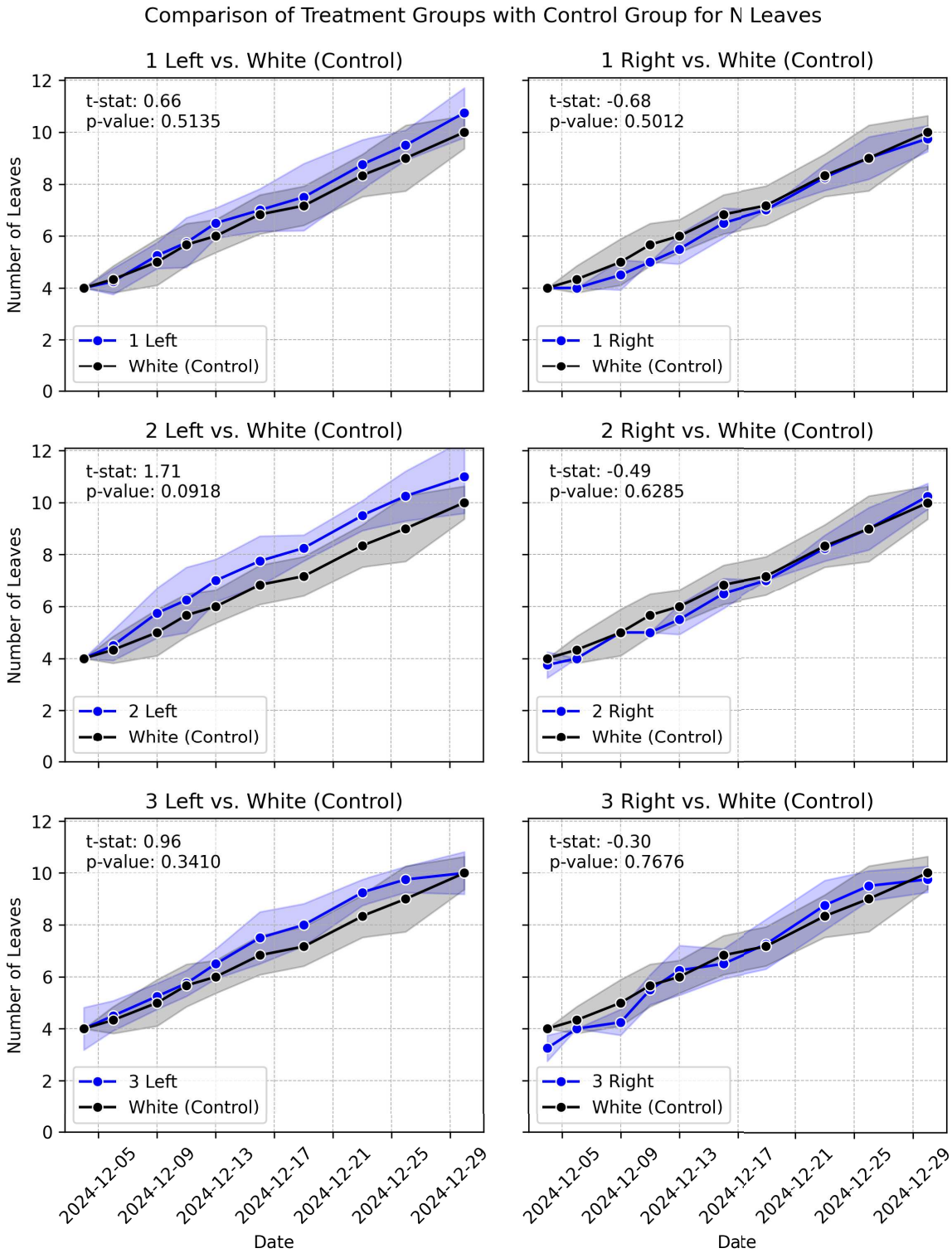

Fig. 12. Average number of leaves over time for each group in the experimental setup.

Biologically, this lack of difference may indicate that under the conditions of this experiment, the quality of light (spectral composition) was not the main factor that determined the final number of leaves. Leaf number is often regulated by complex developmental and hormonal cues that may require longer exposure or different environmental conditions to manifest measurable differences.

VI. Discussion

This study employed an evolutionary algorithm to optimize the spectral composition of RGB LED lighting for lettuce cultivation. The evolutionary process successfully converged on a dominant light recipe: 67% red, 13% green, and 20% blue. This convergence is, in fact, the central validation of the

GA methodology. The experiment was designed to test if the GA could autonomously discover a state-of-the-art recipe from a neutral, full-spectrum baseline (the cold-white LED). Its success is confirmed by this final recipe being consistent with established plant photobiology [35]. The process was not a linear progression, as fitness values are only comparable within a single generation, but the consistent reselection of high-red individuals demonstrates the effectiveness of the selection pressure.

It is important to acknowledge that this physical-in-the-loop design introduces a temporal dependence: the physiological state of the crops in any given generation is partially influenced by the light exposure received in the preceding generation. This "carry-over" effect creates a heterogeneous baseline for comparison. To eliminate this variable, an ideal experimental design would necessitate a complete crop replacement strategy, where the plants in the experimental setup are swapped for a fresh cohort of standardized plants, cultivated in a parallel auxiliary setup under identical control conditions, at the onset of each new generation. However, maintaining a continuous supply of plants at the exact same developmental stage for transplantation presents prohibitive logistical and resource constraints.

Despite these constraints, the findings demonstrate the GA's robustness in handling a complex, noisy, multivariable problem. It is crucial to clarify that the six lighting zones were not independent experiments but comprised the population for a single GA run. The fact that the algorithm successfully converged on a stable, high-performing light recipe, despite environmental noise and cumulative developmental effects, suggests that the proposed methodology is viable for real-world adaptive systems. Finally, the lack of significant yield (weight) improvement should not be interpreted as a failure, but rather, it highlights the GA's strength in optimizing a weighted-sum fitness function across four distinct traits to find the best overall balance, rather than maximizing a single metric.

Analyzing the individual morphological variables provides a more nuanced understanding of the effects of the optimized light recipes. The data from the *t*-tests and comparison plots for each variable reveal specific responses that were not evident from the overall fitness score alone. While the final average biomasses for most RGB treatments were numerically higher than for the control group, the statistical analysis revealed no significant difference between any of the treatment groups and the cold-white LED control. The *p*-values for all biomass comparisons were well above the 0.05 significance threshold. This suggests that while certain spectral compositions may have promoted slightly more biomass accumulation, the effect was not consistent enough to be statistically significant, possibly due to a combination of high biological variability and a small sample size. Therefore, while the optimized light recipe (67:13:20) from the evolutionary process was the best performer, it did not lead to a statistically significant increase in biomass compared to the control condition.

In contrast to plant biomass, the analysis of plant height yielded statistically significant results. Four of the six RGB lighting zones (1 Left, 1 Right, 2 Left, and 2 Right) showed a notable increase in height compared to the control group ($p < 0.05$). However, from a horticultural perspective, this increase must be interpreted with caution. While it suggests a photomorphogenic response, it is likely indicative of a shade-avoidance syndrome (SAS) or etiolation, potentially driven by insufficient light intensity or the specific spectral quality (such as the red:blue ratio) in those zones. Unlike biomass accumulation, this elongation does not necessarily represent a desirable growth outcome, as energy is diverted toward stem elongation to seek light rather than leaf expansion. The observation that the recipes in Zone 1 (which produced the tallest plants) had distinct spectral compositions compared to the control supports the conclusion that the light environment triggered this morphological adaptation. The lack of a significant height difference in Group 3, despite its high red light proportion (67% and 83%), further suggests that the relationship between spectrum and height is nonlinear and heavily influenced by the total photon flux received by the plant.

The results for plant width were more limited. Only one treatment group (2 Left) showed a statistically significant increase in width compared to the control group ($p = 0.0444$). The marginal *p*-values for other groups (e.g., 2 Right and 3 Left) suggest a potential trend, but one that was not strong enough to be conclusive in this experiment. The statistically significant increase in width in lighting zone 2 Left, with its final spectral composition of 30:15:55, points toward the potential importance of a higher proportion of blue light for promoting lateral growth and leaf expansion.

The most consistent result across all treatments was the lack of any significant difference in the number of leaves. The *p*-values for all comparisons were far above the 0.05 significance level, indicating that none of the tested light recipes significantly influenced the rate of leaf initiation. This suggests that for lettuce, leaf count may be a more stable metric, less sensitive to changes in spectral quality over this 25-day growth period.

The GA proved effective in identifying a promising light recipe (67% red, 13% green, and 20% blue) that performed optimally within the constraints of the experiment. However, the subsequent statistical analysis of individual plant variables revealed a more complex picture. While different light treatments did not lead to significant changes in plant weight or leaf count, they had a clear and significant effect on plant height and, in one specific case, width. This divergence between the overall fitness score and the statistical significance of individual variables highlights the importance of a multifaceted approach to evaluating crop performance. The results suggest that the ideal light recipe is highly dependent on the specific growth trait being prioritized—whether it be increased height for certain ornamental plants or enhanced lateral growth for leafy greens. Future research could focus on refining the GA's fitness function to weigh specific variables more heavily, allowing for the optimization of light recipes for targeted crop characteristics.

It is important to address the study's claims regarding resource-use efficiency. While this study successfully developed a GA-driven methodology to optimize spectral composition for morphological traits, we did not conduct a final

quantitative analysis of the resulting LUE or the overall electrical efficiency. This study's contribution toward sustainability is, therefore, the methodology itself—a framework designed to find a recipe that should, in principle, improve LUE by maximizing growth under an identical PPFD. However, a complete validation would require a direct energy analysis. This would involve measuring the specific electrical power consumption (in watts) of the RGB fixtures when producing the optimal (67:13:20) ratio versus the power consumption of the cold-white LED control, all while maintaining the same 200-μmol/m^2 . s^{-1} PPFD. From there, the final LUE (g . mol^{-1}) for both the optimized and control groups could be calculated and compared. This direct quantification was a limitation of this study and remains a critical next step to validate the true energy-saving potential of the optimized recipe.

VII. Conclusion

This study introduces a bio-inspired optimization algorithm to refine the light energy spectral composition of RGB LED using a GA, incorporating key morphological attributes (height, width, weight, and the number of leaves) to enhance crop performance. The algorithm employs evolutionary processes such as selection, crossover, and mutation to iteratively converge toward spectral distributions that optimize plant growth under controlled conditions.

The optimization process consistently favored a spectral composition of approximately 67% red, 13% green, and 20% blue, aligning with previous findings on photosynthetic efficiency and light-use optimization. Notably, while the algorithm identified this balance as optimal, the experimental results revealed that plant height was the most responsive parameter to RGB lighting, showing statistically significant increases under multiple treatments. In contrast, no significant effects were observed for weight or number of leaves, and width showed only one significant improvement among the six treatment groups. These findings indicate that spectral composition has a measurable effect on crop architecture, particularly elongation, but a limited impact on overall biomass or lateral development under the tested conditions.

Additional insights point to the importance of interpreting GA fitness values within the context of each generation, as performance gains are local rather than absolute. Observed inconsistencies in the light energy spectral composition of the RGB LEDs, despite similar conditions, suggest the influence of microclimatic variations, possibly due to minor ventilation differences, underscoring the value of zone-specific environmental monitoring.

While the proposed methodology offers a robust framework for the spectral compositions optimization of RGB LEDs light energies, it assumes constant PPFD and DLI across all growth stages, which may not be ideal for dynamic plant physiology. Moreover, as this study was limited to lettuce, broader validation is needed across different crop species and phenological stages.

Future work should explore real-time dynamic spectral modulation and the incorporation of additional spectral components such as far-red and UV light. In addition, expanding the optimization framework to include environmental and explicit energy-use parameters, such as direct LUE (g . mol^{-1}) and fixture power consumption (W), could further improve its applicability. We acknowledge that the GA, as implemented in this study, is a long-term optimizer and is not suited for high-frequency, real-time control due to its computational cost and the inherent biological latency required for fitness evaluation.

Therefore, a more feasible future direction would be a hybrid control system. In this architecture, the GA would operate as a high-level, offline optimizer to periodically determine the optimal spectral setpoints (as demonstrated in this work). A separate, lightweight, and computationally efficient algorithm (such as a fuzzy logic controller or a pretrained neural network) would then handle the low-level, fast-acting real-time modulation to adapt to transient environmental changes.

References

[1] FAO, *The State of Food and Agriculture 2023*, FAO, Rome, Italy, Nov. 2023.

[2] *The State of Food and Agriculture 2022*, FAO, Rome, Italy, Nov. 2022.

[3] United Nations, Department of Economic, and Social Affairs, Population Division, *World Population Prospects 2022: Summary of Results*, United Nations, New York, NY, USA, 2022.

[4] FAO, *Urban and Peri-Urban Agriculture Sourcebook*, FAO, Rome, Italy, Jun. 2022.

[5] *The State of Food Security and Nutrition in the World 2023*, Revealing the true cost of food to transform agrifood systems, FAO, Rome, Italy, Jul. 2023.

[6] X. Wang, V. Onychko, V. Zubko, Z. Wu, and M. Zhao, "Sustainable production systems of urban agriculture in the future: A case study on the investigation and development countermeasures of the plant factory and vertical farm in China," *Frontiers Sustain. Food Syst.*, vol. 7, Apr. 2023, Art. no. 973341.

[7] T. Kozai, G. Niu, and M. Takagaki Eds., *Plant Factory: An Indoor Vertical Farming System for Efficient Quality Food Production*, 2nd ed. San Diego, CA, USA: Academic Press, 2020.

[8] K. Benke and B. Tomkins, "Future food-production systems: Vertical farming and controlled-environment agriculture," *Sustainability: Sci., Pract. Policy*, vol. 13, no. 1, pp. 13–26, Jan. 2017.

[9] D. Touliatos, I. C. Dodd, and M. McAinsh, "Vertical farming increases lettuce yield per unit area compared to conventional horizontal hydroponics," *Food Energy Secur.*, vol. 5, no. 3, pp. 184–191, Aug. 2016.

[10] F. Kalantari, O. M. Tahir, R. A. Joni, and E. Fatemi, "Opportunities and challenges in sustainability of vertical farming: A review," *J. Landscape Ecol.*, vol. 11, no. 1, pp. 35–60, Jan. 2018.

[11] T. Van Gerrewey, N. Boon, and D. Geelen, "Vertical farming: The only way is up?," *Agronomy*, vol. 12, no. 1, p. 2, Dec. 2021.

[12] S. Eichelsbacher et al., "What is the limit of vertical farming productivity?," *Food Energy Secur.*, vol. 14, no. 2, Mar. 2025, Art. no. e70061.

[13] S. H. van Delden et al., "Current status and future challenges in implementing and upscaling vertical farming systems," *Nature Food*, vol. 2, no. 12, pp. 944–956, Dec. 2021.

[14] F. A. Lubna, D. C. Lewus, T. J. Shelford, and A.-J. Both, "What you may not realize about vertical farming," *Horticulturae*, vol. 8, no. 4, p. 322, Apr. 2022.

[15] P. Morella, M. P. Lambán, J. Royo, and J. C. Sánchez, "Vertical farming monitoring: How does it work and how much does it cost?," *Sensors*, vol. 23, no. 7, p. 3502, Mar. 2023.

[16] I. Vîrtosu and C. Li, "Vertical farming perspective and challenges: A comparative review between China and the EU," in *Proc. Central Eastern Eur. eDem eGov Days*, Sep. 2024, pp. 1–12.

[17] C. Sowmya, M. Anand, C. Indu Rani, G. Amuthaselvi, and P. Janaki, "Recent developments and inventive approaches in vertical farming," *Frontiers Sustain. Food Syst.*, vol. 8, Sep. 2024, Art. no. 1400787.

[18] J. Pereira and M. G. Gomes, "Lighting strategies in vertical urban farming for enhancement of plant productivity and energy consumption," *Appl. Energy*, vol. 377, Jan. 2025, Art. no. 124669.

[19] C.-S. Lin, C.-C. Yen, C.-S. Shyu, and H.-C. Tsao, "Agriculture with energy conservation and AI technology: Analysis of operational efficiency of vertical farms," *J. Internet Technol.*, vol. 25, no. 7, pp. 1023–1034, Dec. 2024.

[20] R. G. Alves, F. Lima, Ì. M. R. Guedes, and S. P. Gimenez, "Dynamic light optimization in vertical farming using an IoT-driven digital twin framework and artificial intelligence," *Appl. Soft Comput.*, vol. 174, Apr. 2025, Art. no. 112985.

[21] M. J. Usigbe, S. Asem-Hiablie, D. D. Uyeh, O. Iyiola, T. Park, and R. Mallipeddi, "Enhancing resilience in agricultural production systems with AI-based technologies," *Environ., Develop. Sustainability*, vol. 26, no. 9, pp. 21955–21983, Aug. 2023.

[22] A. S. Rathor, S. Choudhury, A. Sharma, P. Nautiyal, and G. Shah, "Empowering vertical farming through IoT and AI-driven technologies: A comprehensive review," *Heliyon*, vol. 10, no. 15, Aug. 2024, Art. no. e34998.

[23] S. Erekath, H. Seidlitz, M. Schreiner, and C. Dreyer, "Food for future: Exploring cutting-edge technology and practices in vertical farm," *Sustain. Cities Soc.*, vol. 106, Jul. 2024, Art. no. 105357.

[24] D. Despommier, "Farming up the city: The rise of urban vertical farms," *Trends Biotechnol.*, vol. 31, no. 7, pp. 388–389, Jul. 2013.

[25] D. Despommier, M. Carter, and G. Giacomelli, *The Vertical Farm: Feeding the World in the 21st Century*. New York, NY, USA: St. Martin's Publishing Group, 2010.

[26] M. Dutta and D. Gupta, "Revolutionizing agriculture: Sustainable solutions for high-yield farming using vertical hydroponics," *GMSARN Int. J.*, vol. 19, pp. 95–106, Jan. 2025.

[27] K. Al-Kodmany, "The vertical farm: A review of developments and implications for the vertical city," *Buildings*, vol. 8, no. 2, p. 24, Feb. 2018.

[28] R. R. Shamshiri et al., "Advances in greenhouse automation and controlled environment agriculture: A transition to plant factories and urban agriculture," *Int. J. Agricult. Biol. Eng.*, vol. 11, no. 1, pp. 1–22, 2018.

[29] TIME. *AeroFarms: The 100 Best Inventions of 2019*. Accessed: Apr. 21, 2025. [Online]. Available: https://time.com/collection/best-inventions-2019/5733085/aerofarms/

[30] F. Bantis, S. Smirnakou, T. Ouzounis, A. Koukounaras, N. Ntagkas, and K. Radoglou, "Current status and recent achievements in the field of horticulture with the use of light-emitting diodes (LEDs)," *Scientia Horticulturae*, vol. 235, pp. 437–451, May 2018.

[31] M. Pessarakli, "Plant responses to extended photosynthetically active radiation (EPAR)," *Adv. Plants Agricult. Res.*, vol. 7, no. 3, p. 313, Aug. 2017.

[32] S. Zhen, M. van Iersel, and B. Bugbee, "Why far-red photons should be included in the definition of photosynthetic photons and the measurement of horticultural fixture efficacy," *Frontiers Plant Sci.*, vol. 12, Jun. 2021, Art. no. 693445.

[33] S. Zhen and B. Bugbee, "Far-red photons have equivalent efficiency to traditional photosynthetic photons: Implications for redefining photosynthetically active radiation," *Plant*, vol. 43, no. 5, pp. 1259–1272, May 2020.

[34] (2022). *ANSI/ASABE S640 JUL2017 (R2022)—Quantities and Units of Electromagnetic Radiation for Plants (Photosynthetic Organisms)*. [Online]. Available: https://webstore.ansi.org/standards/asabe/ansiasabes640jul2017r2022

[35] I. F. Boros, G. Székely, L. Balázs, L. Csambalik, and L. Sipos, "Effects of LED lighting environments on lettuce (Lactuca sativa L.) in PFAL systems—A review," *Scientia Horticulturae*, vol. 321, Nov. 2023, Art. no. 112351.

[36] E. Heuvelink, S. Hemming, and L. F. M. Marcelis, "Some recent developments in controlled-environment agriculture: On plant physiology, sustainability, and autonomous control," *J. Horticultural Sci. Biotechnol.*, vol. 100, no. 5, pp. 604–614, Sep. 2025.

[37] J. Shin and E. S. Runkle, "Considerations of utilizing far-red light in the production of leafy-green vegetables indoors," *Eur. J. Horticultural Sci.*, vol. 89, no. 4, pp. 1–9, Nov. 2024.

[38] N. Budavári, Z. Pék, L. Helyes, S. Takács, and E. Nemeskéri, "An overview on the use of artificial lighting for sustainable lettuce and microgreens production in an indoor vertical farming system," *Horticulturae*, vol. 10, no. 9, p. 938, Sep. 2024.

[39] M. Gargaro, R. J. Murphy, and Z. M. Harris, "Let-us investigate; a meta-analysis of influencing factors on lettuce crop yields within controlled-environment agriculture systems," *Plants*, vol. 12, no. 14, p. 2623, Jul. 2023.

[40] Q. Meng, N. Kelly, and E. S. Runkle, "Substituting green or far-red radiation for blue radiation induces shade avoidance and promotes growth in lettuce and kale," *Environ. Exp. Botany*, vol. 162, pp. 383–391, Jun. 2019.

[41] L. Carotti et al., "Plant factories are heating up: Hunting for the best combination of light intensity, air temperature and root-zone temperature in lettuce production," *Frontiers Plant Sci.*, vol. 11, Jan. 2021.

[42] W. Jin, J. L. Urbina, E. Heuvelink, and L. F. M. Marcelis, "Adding far-red to red-blue light-emitting diode light promotes yield of lettuce at different planting densities," *Frontiers Plant Sci.*, vol. 11, Jan. 2021, Art. no. 609977.

[43] F. Valdez, P. Melin, and O. Castillo, "An improved evolutionary method with fuzzy logic for combining particle swarm optimization and genetic algorithms," *Appl. Soft Comput.*, vol. 11, no. 2, pp. 2625–2632, Mar. 2011.

[44] Y.-T. Kao and E. Zahara, "A hybrid genetic algorithm and particle swarm optimization for multimodal functions," *Appl. Soft Comput.*, vol. 8, no. 2, pp. 849–857, Mar. 2008.

[45] C. A. C. Coello, G. B. Lamont, and D. A. V. Veldhuizen, *Evolutionary Algorithms for Solving Multi-Objective Problems (Genetic and Evolutionary Computation)*. Cham, Switzerland: Springer, Sep. 2007.

[46] C. Darwin, "Origin of the species," in *British Politics and the Environment in the Long Nineteenth Century*. Evanston, IL, USA: Routledge, 2023, pp. 47–55.

[47] G. Zames, "Genetic algorithms in search, optimization and machine learning," *Inf. Technol. J.*, vol. 3, no. 1, p. 301, 1981.

[48] D. B. Fogel, *Artificial Intelligence Through Simulated Evolution*. Hoboken, NJ, USA: Wiley, 1998.

[49] A. Slowik and H. Kwasnicka, "Evolutionary algorithms and their applications to engineering problems," *Neural Comput. Appl.*, vol. 32, no. 16, pp. 12363–12379, Aug. 2020.

[50] S. N. Sivanandam and S. N. Deepa, *Introduction to Genetic Algorithms*. Berlin, Germany: Springer, 2007.

[51] S. Katoch, S. S. Chauhan, and V. Kumar, "A review on genetic algorithm: Past, present, and future," *Multimedia Tools Appl.*, vol. 80, no. 5, pp. 8091–8126, Feb. 2021.

[52] Y. Huang, Y. Lan, S. J. Thomson, A. Fang, W. C. Hoffmann, and R. E. Lacey, "Development of soft computing and applications in agricultural and biological engineering," *Comput. Electron. Agricult.*, vol. 71, no. 2, pp. 107–127, May 2010.

[53] F. K. Shaikh, S. Karim, S. Zeadally, and J. Nebhen, "Recent trends in Internet-of-Things-enabled sensor technologies for smart agriculture," *IEEE Internet Things J.*, vol. 9, no. 23, pp. 23583–23598, Dec. 2022.

[54] N. N. Misra, Y. Dixit, A. Al-Mallahi, M. S. Bhullar, R. Upadhyay, and A. Martynenko, "IoT, big data, and artificial intelligence in agriculture and food industry," *IEEE Internet Things J.*, vol. 9, no. 9, pp. 6305–6324, May 2022.

[55] *About FIWARE–FIWARE*, FIWARE, Berlin, Germany, Oct. 2021.

[56] S. K. Roy, S. Misra, N. S. Raghuwanshi, and S. K. Das, "AgriSens: IoT-based dynamic irrigation scheduling system for water management of irrigated crops," *IEEE Internet Things J.*, vol. 8, no. 6, pp. 5023–5030, Mar. 2021.

[57] C. Kamienski et al., "Smart water management platform: IoT-based precision irrigation for agriculture," *Sensors*, vol. 19, no. 2, p. 276, Jan. 2019.

[58] R. G. Alves, R. F. Maia, and F. Lima, "Development of a digital twin for smart farming: Irrigation management system for water saving," *J. Cleaner Prod.*, vol. 388, Feb. 2023, Art. no. 135920.

[59] J. Zhang and D. Tao, "Empowering things with intelligence: A survey of the progress, challenges, and opportunities in artificial intelligence of things," *IEEE Internet Things J.*, vol. 8, no. 10, pp. 7789–7817, May 2021.

[60] M. Lu, H. Liu, Y. Yang, H. Li, P. Gao, and J. Hu, "Multi-objective optimization and decision-making of low-carbon environmental parameters in AIoT-enabled controlled environment agriculture," *IEEE Internet Things J.*, vol. 12, no. 23, pp. 49160–49173, Dec. 2025.

[61] M. Singh, K. S. Sahoo, and A. H. Gandomi, "An intelligent-IoT-based data analytics for freshwater recirculating aquaculture system," *IEEE Internet Things J.*, vol. 11, no. 3, pp. 4206–4217, Feb. 2024.

[62] B. L. Welch, "The generalization of 'student's' problem when several different population variances are involved," *Biometrika*, vol. 34, nos. 1–2, pp. 28–35, Jan. 1947. [Online]. Available: http://www.jstor.org/stable/2332510

Rafael Gomes Alves received the B.S. and M.S. degrees in mechanical engineering from the Centro Universitário FEI, São Bernardo do Campo, São Paulo, Brazil, in 2017 and 2020, respectively, where he is currently pursuing the Ph.D. degree in electrical engineering.

From 2017 to 2020, he participated in the "Smart Water Management Platform" (SWAMP) Project funded by European Commission. Since 2023, he has been working in the "Traceable Smart Products and Interoperability in the Automotive Industry Supply Chain With the Application to Sensorized Tires—Tire IoT" Project as an Independent Technical Consultant. He is currently an Assistant Professor with the Centro Universitário FEI. His research interests include digital twins applied to agriculture and controlled environment agriculture.

Fábio Lima (Member, IEEE) received the B.Sc. degree in electrical engineering from Paulista State University (UNESP), São Paulo, Brazil, in 1998, and the M.Sc. and Ph.D. degrees in electrical engineering from the University of São Paulo (USP), São Paulo, Brazil, in 2001 and 2010, respectively.

He is a Full-Time Professor with the Industrial Engineering Department, Centro Universitário FEI (FEI), São Paulo, where he teaches subjects related to industrial automation and manufacturing systems. He is also a member of the Master's Degree Program in mechanical engineering with FEI in the production systems area. He is currently the Coordinator of the Digital Manufacturing Laboratory and the 5G Solutions Center, FEI, developing projects related to Industry 4.0.

Dr. Lima is a Scientific Adviser to FAPESP (São Paulo Research Foundation), Brazil, and a member of the IEEE Industrial Electronics Society. His presentations at IEEE-IECON conferences in 2013 (Vienna) and 2015 (Yokohama) won the Best Presentation Award.

Ítalo Moraes Rocha Guedes received the B.S. degree in agronomy from the Federal University of Paraíba (UFPB), João Pessoa, Brazil, in 1999, and the M.Sc. degree in crop science and the D.Sc. degree in soil science and plant nutrition from the Federal University of Viçosa (UFV), Viçosa, Brazil, in 2003 and 2008, respectively.

He has been a Researcher with Brazilian Agricultural Research Corporation (Embrapa Hortaliças), Brasília, Brazil, since December 2008. His research focuses on plant mineral nutrition and soilless cultivation systems in protected and controlled environments.

Dr. Guedes served as the Chair of the Management Committee of Embrapa's Corporate Vegetable Research Portfolio, from 2019 to 2020. He coordinated the first project by Brazilian Public Research Institution to develop a plant production system for vertical farms, from 2020 to 2024.

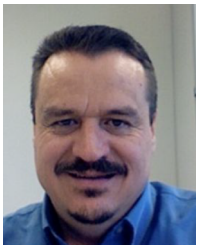

Salvador Pinillos Gimenez (Senior Member, IEEE) was born in São Paulo, Brazil, in 1962. He received the Graduate degree in electrical engineering from UMC, São Paulo, in 1984, the M.S. degree in electrical engineering from the Microelectronics Laboratory, LME, University of São Paulo, São Paulo, in 1990, and the Ph.D. degree in electrical engineering from the Integrated Systems Laboratory, LSI, University of São Paulo, in 2004.

From 1987 to 1993, he worked as a Product Engineer with Dimep S.A. São Paulo, Brazil, and Tracecom Telecommunications Systems, São Paulo, Brazil. In 1994, he joined Ford (Electronic Division, after Visteon), Guarulhos, São Paulo, as a Component Engineer, a Supply Quality Assurance, and a Quality and Productivity Coordinator. Since 1999, he has been a Full Professor and a Researcher with the FEI University Center, São Paulo. He has authored textbooks on microcontrollers and holds industrial patents on MOSFET with innovative layout styles. His major fields of study include novel nonstandard MOSFET structures, analog and digital CMOS IC designs, and evolutionary electronics by developing analog and radio frequency CMOS IC optimization tools based on heuristic algorithms of artificial intelligence.

Dr. Gimenez is a member of the Microelectronic Brazilian Society (SBMicro). Since October 2015, he has been on the editorial board (Associate Editor) of the *Electronics Letters* journal (Institution of Engineering and Technology, IET—England, Wales, and Scotland) and the *Journal of Integrated Circuits and Systems* since 2020.

Coordenação de A perfeiçoamento de Pessoal de Nível Superior (CAPES) - ROR identifier: 00x0ma614